

# A Comparative Study of Oxo-Ligand Effects in the Gas-Phase Chemistry of Atomic Lanthanide and Actinide Cations

Hans H. Cornehl, Ralf Wesendrup, Martin Diefenbach, and Helmut Schwarz\*

**Abstract:** The effects of oxo ligands on lanthanide and actinide cations have been examined for the mono- and dioxocations  $\text{MO}^+$  and  $\text{MO}_2^+$  of cerium, neodymium, thorium, and uranium by probing C–H and C–C bond activation of hydrocarbons in an FT–ICR mass spectrometer. The metal monoxide cations are readily available by reaction of the “bare” metal cations with  $\text{O}_2$ ,  $\text{CO}_2$ ,  $\text{N}_2\text{O}$ , or  $\text{H}_2\text{O}$ . In the ensuing oxidation of  $\text{MO}^+$ ,  $\text{UO}_2^+$  is obtained by each of these oxidants, while  $\text{CeO}^+$  could only be oxidized by  $\text{N}_2\text{O}$ .

$\text{NO}_2$  was necessary for the generation of  $\text{ThO}_2^+$ , and  $\text{NdO}_2^+$  could not be prepared at all. The monoxides are rather unreactive and only dehydrogenate reactive substrates such as 1-butene and 1,4-cyclohexadiene to generate the corresponding butadiene or benzene complexes. In con-

trast,  $\text{CeO}_2^+$  and  $\text{ThO}_2^+$  react efficiently with different substrates by abstraction of a hydrogen atom and formation of the closed-shell species  $\text{OMOH}^+$ , or by oxygen atom transfer to unsaturated hydrocarbons. In marked contrast,  $\text{UO}_2^+$  only undergoes very slow adduct formation with unsaturated hydrocarbons. The results are compared with the reactions of the “bare” metals with respect to the influence of the oxo ligand as well as to the underlying electronic features of the investigated complexes.

## Keywords

actinides · C–H activation · lanthanides · mass spectrometry · metal oxides · oxygen transfer

## Introduction

Within the last decade gas-phase investigations of “bare” transition-metal cations have developed as an independent and fascinating area of contemporary research.<sup>[1]</sup> These experiments provide the possibility of probing the intrinsic properties of the metals without interference by bulk effects which are present in condensed systems. Thus, a comprehensive body of information on thermochemistry, kinetics, and mechanistic aspects of transition-metal chemistry in the gas phase is now available. Recently, this work has been extended to the f-elements<sup>[2]</sup> by systematic studies on the reactions of the whole series of lanthanide cations  $\text{Ln}^+$  with various organic substrates.<sup>[3]</sup> These experiments revealed that at least two non-f electrons in the ground-state configuration of  $\text{Ln}^+$  are required for the activation of alkanes, whereas the corelike 4f electrons do not participate in bond formation.<sup>[2c]</sup> Hence, the chemistry of lanthanides, which do not possess two non-f electrons in their ground state, is determined by the promotion energy of a 4f electron into a non-f orbital. Unfortunately, a comparative systematic study of the actinide elements is prevented by their radioactivity, unless strict supplementary safety requirements are met, which are not provided in a standard laboratory. But case studies revealed that the higher

homologues of cerium and neodymium, the 5f-elements thorium<sup>[4]</sup> and uranium,<sup>[5]</sup> with electronic ground-state configurations of  $(7s^1 6d^2)$  and  $(7s^2 5f^3)$ , respectively, do effectively dehydrogenate saturated hydrocarbons, in complete agreement with the rule derived for the lanthanides. As an extension to the investigation of the “bare” metal cations, the evaluation of ligand effects adds valuable information. Addition of one or several ligands L may well be regarded as an attempt to establish a link between gas-phase and condensed-phase chemistry and can provide a rationale for the way in which the reactivity of  $\text{ML}^+$  complexes changes as compared with the “bare” transition-metal cations  $\text{M}^+$ .<sup>[6]</sup>

A common feature of all f-elements is their high oxophilicity, so it appears to be a logical extension to previous work to study the corresponding metal-oxide cations. The chemistry of diatomic metal oxocations  $\text{MO}^+$  has recently been reviewed with an emphasis on the first transition-metal row.<sup>[7]</sup> These studies, together with theoretical and experimental investigations of transition-metal dioxides,<sup>[8]</sup> showed that the oxygen atom is far from serving as a simple spectator ligand. It strongly influences the electronic structure of the metal center and thus dramatically changes its chemistry. For the f-elements, analogous effects have recently been reported in an investigation of  $\text{CeO}_n^+$  ( $n = 0-2$ ), as an example.<sup>[9]</sup>

The present paper focuses on the effects of oxo ligands on the chemical reactivity of the actinides Th and U in comparison with their lanthanide homologues Ce and Nd, as probed by a set of selected hydrocarbon substrates. This comparison of the ac-

[\*] H. Schwarz, H. H. Cornehl, R. Wesendrup, M. Diefenbach  
Institut für Organische Chemie der Technischen Universität Berlin  
Strasse des 17. Juni 135, D-10623 Berlin (Germany)  
Fax: Int. code +(30)314-21102

tinide and the lanthanide rows is expected to yield valuable information concerning the role of f electrons in chemical processes. For this purpose, in the following discussion data from earlier investigations of the “bare” metal cations, obtained with an identical experimental setup, are also included.

## Experimental Section

The experiments were performed with a Spectrospin CMS 47X FT-ICR mass spectrometer equipped with an external ion source and a superconducting magnet (Oxford Instruments, 7.05 T); the instrument and its operation have been described in detail previously.<sup>[10]</sup> In brief,  $M^+$  ions were generated with laser desorption/laser ionization by focusing the beam of an Nd:YAG laser (1064 nm) onto a pure metal target.<sup>[11]</sup> The cations were extracted from the ion source and transferred to the analyzer cell by a system of electric potentials and lenses. Isolation of the most abundant metal isotope and all subsequent isolation steps were performed by using FERETS,<sup>[12]</sup> a computer-controlled ion-ejection protocol that combines single-frequency ion-ejection pulses with frequency sweeps to optimize ion isolation. Most oxo- and dioxocations were generated by treating the “bare” metal ions with pulsed-in carbon dioxide or nitrous oxide, respectively. For the generation of  $CeO_2^+$  consecutive pulses of carbon dioxide and nitrogen dioxide were used (see below). Thermalization and removal of excess energy were afforded by collisions with excess reactant gas (maximum pressure ca.  $10^{-4}$  mbar), and the thermalized ions were carefully reisolated to avoid off-resonance excitation.<sup>[13]</sup> Reactants were admitted to the cell through a leak valve at a stationary pressure of  $10^{-8}$ – $10^{-7}$  mbar. Rate constants were derived from the pseudo first-order decay of the reactant ions, corrected for undesired reactions with residual water, and are reported with an estimated error of  $\pm 40\%$ , using the theoretical collision rate according to the average dipole orientation theory ( $k_{Ado}$ ) as a reference.<sup>[14]</sup> Collision-induced dissociation (CID)<sup>[15]</sup> experiments were carried out at different excitation energies with argon as collision gas at a pressure of  $10^{-7}$  mbar. All functions of the instrument were controlled by a Bruker Aspect 3000 minicomputer.

All reactions of  $ThO_2^+$  with hydrocarbons were investigated by using perdeuterated compounds. Severe interference due to the reaction of the dioxo cation with residual water to yield  $ThO_2H^+$ , a product which also results from the hydrocarbon reactions, did not allow for a proper reaction analysis with non-deuterated compounds. Water is not only present as an almost constant background impurity in the machine, but also in variable amounts in the valves used for pulsing and leaking-in the reactants. Thus, a correction for the background reaction by means of a “blind-probe” with argon, as performed for the case of  $CeO_2^+$ ,<sup>[9]</sup> was not possible here.

Ab initio pseudopotential (PP) calculations were performed on  $ThO^+$  and its fragments  $Th^+$  and O with the quasirelativistic 60-core electron thorium PP and the associated  $(12s\ 11p\ 10d\ 8f)/[8s\ 7p\ 6d\ 4f]$  valence basis set by Küchle et al.<sup>[16]</sup> A  $(14s\ 9p\ 4d)/[6s\ 5p\ 3d]$  atomic natural orbital (ANO) basis set was used for oxygen.<sup>[17]</sup> Spin-restricted Hartree–Fock computations were followed by spin-restricted coupled-cluster calculations, as implemented in MOL-PRO96,<sup>[18]</sup> covering all single and double excitations, and a perturbational treatment of triple excitations to account for electron correlation (CCSD(T)).<sup>[19]</sup> with correlation of all explicitly treated electrons except for the 5s, 5p, and 5d electrons of thorium and the 1s electrons of oxygen. Geometries were optimized stepwise by calculating several points in the proximity of the minima on the potential-energy surfaces. Further, state-averaged complete active space self-consistent field (CASSCF) calculations were performed to obtain access to higher excited states, in particular the  $^2\Phi$  state for  $ThO^+$  within the  $C_{2v}$  symmetry employed here. All energies given are not corrected for zero-point vibrational energies or for thermal effects.

## Results and Discussion

The four f-element cations  $M^+$  under investigation ( $M = Ce, Nd, Th, U$ ) are readily oxidized to the corresponding monoxides  $MO^+$  in exothermic<sup>[20, 21]</sup> (see Table 1) ion/molecule reactions

Table 1. Experimental bond dissociation energies (BDEs) in  $\text{kcal mol}^{-1}$  for oxo- and dioxocations and for oxidizing reagents.

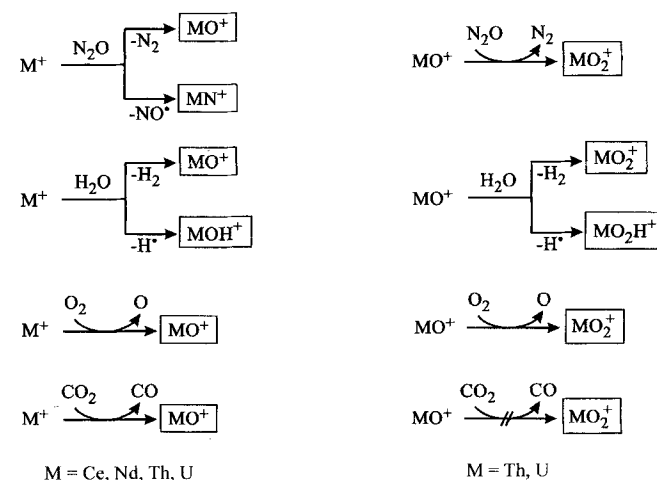
M	BDE( $M^+ - O$ )	BDE( $OM^+ - O$ )	R	BDE(R–O) [b]
Ce	$196 \pm 16$ [b]	$88 \pm 15$ [c]	$N_2$	40.0
Nd	$178 \pm 7$ [a]	$50 \pm 39$ [d]	O	119.2
Th	$209 \pm 4$ [b]	$110 \pm 2$ [e]	CO	127.2
U	$194 \pm 5$ [b]	$181 \pm 3$ [b]	$H_2$	117.4
			NO	73.5

[a] Ref. [20]. [b] Ref. [21]. [c] Ref. [9]. [d] Only this very crude estimate can be derived from ref. [20]. [e] The upper boundary given in ref. [21] has been corrected according to experimental results obtained in this work.

by either nitrous oxide, molecular oxygen, or carbon dioxide (Table 2 and Scheme 1). In the case of  $N_2O$  a substantial fraction of  $MN^+$  is formed as a by-product, whereas for the other two reagents formation of  $MO^+$  represents the only primary

Table 2. Reaction rates relative to  $k_{Ado}$  for the reactions of f-elements with oxidizing reagents. Products correspond to transfer of an oxygen atom from the substrate to the reactant ion unless denoted otherwise. Branching ratios (%) are given in parentheses.

Ion	$O_2$	$CO_2$	$N_2O$ ( $MN^+/MO^+$ )	$H_2O$ ( $MO^+/MOH^+$ )
$Ce^+$	1.05	0.70	1.03 (25/75)	0.20 (50/50)
$Nd^+$	0.80	0.08	0.47 (0/100)	0.10 (90/10)
$Th^+$	1.12	0.95	1.02 (35/65)	0.57 (65/35)
$U^+$	1.17	1.02	1.25 (30/70)	0.47 (100/0)
$CeO^+$	–	–	–	–
$NdO^+$	–	–	–	–
$ThO^+$	–	–	0.71	0.36 ( $ThO_2H^+$ )
$UO^+$	0.95	0.002	0.49	0.04
$ThO_2^+$	–	–	–	0.10 ( $ThO_2H^+$ )



Scheme 1. Formation of  $MO^+$  and  $MO_2^+$ .

product channel. These reactions are driven by the formation of the strong metal–oxygen bonds. In contrast, oxidation of  $M^+$  by water proceeds at significantly lower rates than with carbon dioxide, for instance, even though extrusion of oxygen from water is favored by  $10 \text{ kcal mol}^{-1}$  for the former reagent (Table 1). However, oxidation of  $M^+$  by water requires substantial rearrangement of the substrate’s skeleton to yield  $MO^+$  and  $H_2$ . Moreover, in all cases except for  $M = U$  the hydroxyl complexes  $MOH^+$  are formed as by-products, concomitantly with

the loss of a hydrogen atom, in the primary reaction with water. These findings suggest that for the  $M^+/H_2O$  systems significant barriers, most probably due to the shift of a hydrogen atom with the associated crossing of two different spin hypersurfaces, are operative en route to the  $MO^+$  products.<sup>[22]</sup>

The second oxidation step to yield  $MO_2^+$  is not in all cases as straightforward as the first one:

1)  $CeO_2^+$  can only be formed from  $CeO^+$  with nitrogen dioxide as oxidant. The lower bracket of the bond dissociation energy (BDE) in  $CeO_2^+$  ( $BDE(OCe^+-O) = 88 \pm 15 \text{ kcal mol}^{-1}$ ) has been derived from this reaction.<sup>[9]</sup> However, the oxidation of  $CeO^+$  cannot be achieved by using  $N_2O$  ( $BDE(N_2-O) = 40.0 \text{ kcal mol}^{-1}$ ), which indicates that the barrier for the oxygen transfer is located above the  $CeO^+/N_2O$  entrance channel. In line with their higher BDEs, neither molecular oxygen nor carbon dioxide react with  $CeO^+$ . Water and  $CeO^+$  form a complex of formal composition  $[Ce, O_2, H_2]^+$ , which either corresponds to a genuine  $CeO^+ \cdot H_2O$  adduct complex or to the bishydroxyl species  $Ce(OH)_2^+$ .<sup>[9]</sup>

2) None of the oxidizing reagents examined here was able to form  $NdO_2^+$  in the reaction with  $NdO^+$ , even after the reactant ions had been kinetically excited. However, an upper limit for  $BDE(ONd^+-O)$  cannot be derived from the non-occurrence of these oxidation reactions, since substantial kinetic barriers may be associated with the oxygen transfer process. The crude estimate for  $BDE(ONd^+-O)$  given in Table 1 suggests that oxygen transfer from  $O_2$ ,  $CO_2$ , or  $H_2O$  is not possible on thermochemical grounds.

3) Both  $ThO^+$  and  $UO^+$  are effectively converted to  $ThO_2^+$  and  $UO_2^+$  as sole products in the ion/molecule reactions with  $N_2O$ . Also, water is activated by these two actinide-oxide cations. Since  $ThO^+$  exhibits only one free valence electron, the closed-shell species  $ThO(OH)^+$  is the only product formed in the reaction of the latter ion with water; this implies that  $BDE(OTh^+-OH)$  is greater than  $BDE(H-OH) = 119.2 \text{ kcal mol}^{-1}$ . In fact, formation of  $ThO_2^+$  cannot be observed in the reaction of  $ThO^+$  and water because it would be endothermic by at least  $3 \text{ kcal mol}^{-1}$  (see below). The  $UO^+/H_2O$  system, on the other hand, behaves completely differently. Formation of the dioxide  $UO_2^+$  concomitantly with the loss of molecular hydrogen is the exclusive reaction pathway and is exothermic by as much as  $60 \text{ kcal mol}^{-1}$  (Table 1). This finding is not unexpected and reflects the very stable electronic structure of the uranyl cation.<sup>[23]</sup> Two genuine double bonds are formed between the metal center and the two oxygen ligands, and the nonbonding metal-centered  $5f$  electron gives rise to the  $^2\Phi_u$  ground state of  $UO_2^+$ . As expected from the lower BDE of  $ThO^+-O$  as compared with those of  $O-O$  and  $CO-O$ , these substrates do not react with  $ThO^+$ . In contrast, oxidation of  $UO^+$  by molecular oxygen proceeds at the collision limit, whereas only a very slow reaction is observed with  $CO_2$ . Again, this finding points towards substantial barriers along the oxygen transfer process, because mere thermochemistry would strongly favor formation of  $UO_2^+$  in the reaction of  $UO^+$  with  $CO_2$ . We note in passing that  $ThO_2^+$ , unlike the other dioxo cations, reacts at about 10%  $k_{ADO}$  with water to yield  $ThO(OH)^+$  and the neutral  $OH^{\cdot}$  radical; this has consequences for the experimental proceedings in this case (see Experimental Section). Thus, a lower bracket for  $BDE(ThO_2^+-H)$  can be derived, to

$119 \text{ kcal mol}^{-1}$  ( $BDE(HO-H)$ ) since only exothermic reactions are observed within the experimental setup of an FT-ICR-MS, provided the reactant ions are properly thermalized.

To prove that genuine dioxides are generated within the experimental setup, the CID channels of  $MO_2^+$  ( $M = Th, U$ ; for Ce see ref. [9]) were recorded at different excitation energies. The plot of ion intensities ( $ThO_2^+$ ,  $ThO^+$ ,  $Th^+$ ) versus the uncorrected center of mass energy ( $E_{CM}$ ) is depicted in Figure 1 for

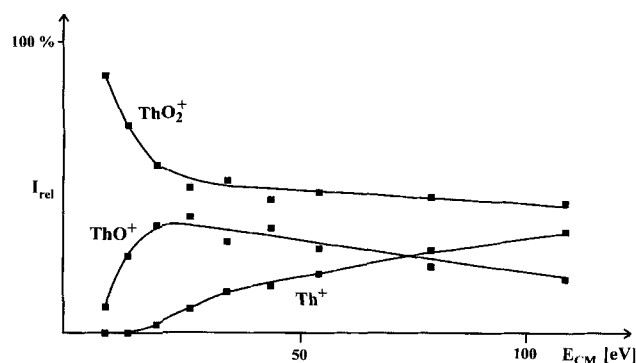


Figure 1. Energy-resolved CID of  $ThO_2^+$  with argon as collision gas ( $10^{-7}$  mbar), yielding  $ThO^+$  as primary and  $Th^+$  as secondary fragment.

the thorium case. Loss of a single oxygen ligand at lower energies and subsequent loss of the second ligand at higher energies clearly indicate the existence of two genuine oxygen ligands bound to the metal center. The results for  $M = U$  exactly parallel those obtained for Th and are in line with recent theoretical investigations.<sup>[23]</sup>

**Reactions of metal dioxocations:** None of the hydrocarbon substrates under investigation were found to be activated by  $UO_2^+$  and even in the case of 1,4-cyclohexadiene only very slow adduct formation to yield  $UO_2C_6H_8^+$  was observed. In fact, recent theoretical as well as experimental investigations<sup>[23]</sup> suggested the complete inertness of this triatomic cation. The  $^2\Phi_u$  ground state of  $UO_2^+$  can be regarded as a closed valence subshell due to formation of two genuine double bonds between the uranium center and the oxygen ligands plus a single nonbonding, metal-centered  $f$  electron. The unpaired  $f$  electron on uranium is not only sterically shielded, but is probably rather compact with respect to its radial expectation value due to the much higher charge on the metal center in  $UO_2^+$  ( $q(U) = 2.32e$ ) as compared with "bare"  $U^+$ .<sup>[23]</sup> Fully in line with this view, determination of the second ionization energy of  $UO_2$  by charge-stripping experiments in a four-sector mass spectrometer<sup>[24]</sup> systematically yields values that are too high, reflecting the ionization of  $UO_2^+$  into an excited state of  $UO_2^{2+}$ .<sup>[25]</sup> Clearly, the  $f$  electron is not detached by the stripping process, which instead removes one of the paired electrons from bonding molecular orbitals that are spatially more accessible.

As mentioned above, the generation of the corresponding lower homologue  $NdO_2^+$  could not be achieved. Therefore, the following discussion focuses on the reactivity of  $ThO_2^+$  towards different hydrocarbon substrates compared with the reactivity of  $CeO_2^+$ .<sup>[9]</sup> Table 3 lists the relative reaction rates of  $MO_2^+$  ( $M = Ce, Th$ ) with several hydrocarbons. Let us neglect to a

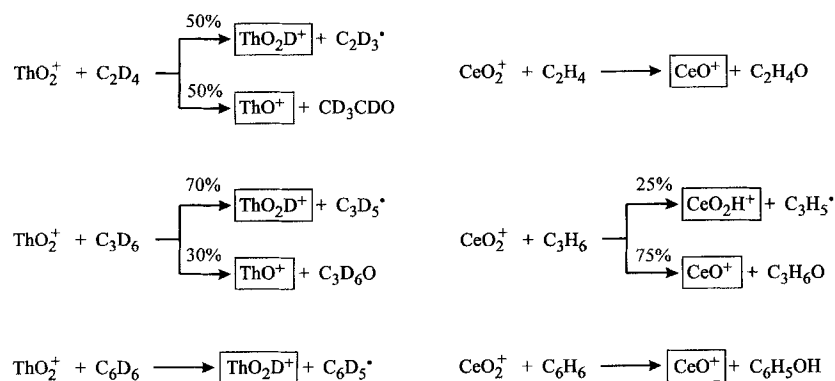
Table 3. Rate constants relative to the theoretical collision rate  $k_{\text{ABO}}$  for reactions of  $\text{MO}_2^+$  ( $M = \text{Ce}, \text{Nd}, \text{Th}, \text{U}; n = 0-2$ ) [a].

	$\text{CH}_4$	$\text{C}_2\text{H}_6$	$\text{C}_3\text{H}_8$	$n\text{-C}_4\text{H}_{10}$	$\text{C}_2\text{H}_4$	$\text{C}_3\text{H}_6$	$\text{C}_6\text{H}_6$	$1\text{-C}_4\text{H}_8$	cyclo- $\text{C}_6\text{H}_8$
$\text{Ce}^+$ [b]	–	0.005	0.45	0.30	1.0	1.0	1.0	1.0	1.0
$\text{Nd}^+$ [b]	–	–	–	–	–	–	–	0.45	1.0
$\text{Th}^+$ [c]	0.04	0.40	0.65	0.65	0.92	1.0	1.0	1.0	1.0
$\text{U}^+$ [d]	–	–	0.02	0.2	1.0	1.0	0.9	0.9	1.0
$\text{CeO}^+$ [e]	–	–	–	–	–	–	–	–	0.004
$\text{NdO}^+$	–	–	–	–	–	–	–	–	0.03
$\text{ThO}^+$	–	–	–	–	–	–	–	0.22	0.75
$\text{UO}^+$	–	–	–	–	–	–	–	0.008	0.51
$\text{CeO}_2^+$ [e]	–	–	0.003	0.10	0.10	0.44	0.64	0.62	
$\text{ThO}_2^+$	–	[f]	0.13 [g]	[f]	0.14 [g]	0.36 [g]	0.54 [g]	[f]	[f]

[a] None of the ions reacts with molecular hydrogen.  $\text{UO}_2^+$  was found to be unreactive towards all substrates under investigation. Generation of  $\text{NdO}_2^+$  was not possible under the experimental conditions chosen. Non-observance of a reaction is denoted by a dash and corresponds to  $k_{\text{rel}} < 0.001$ . [b] Ref. [3], except for  $\text{Ce}^+/\text{C}_6\text{H}_6$  (ref. [9]) and  $\text{Nd}^+/\text{C}_6\text{H}_6$  (this work). [c] Ref. [4], except for  $\text{Th}^+/\text{C}_6\text{H}_6$  (this work, exclusive formation of  $\text{ThC}_6\text{H}_6^+$ ) and  $\text{Th}^+/\text{cyclo-C}_6\text{H}_8$  (this work; exclusive formation of  $\text{ThC}_6\text{H}_8^+$ ). With regard to the inherent systematic error in determination of absolute rate constants, we remeasured the reaction of  $\text{Th}^+$  with propene and corrected the values from ref. [4] by a factor of 2 for better comparison. [d] Ref. [5], except for  $\text{U}^+/\text{cyclo-C}_6\text{H}_8$  (this work; exclusive formation of  $\text{UC}_6\text{H}_8^+$ ) [e] Ref. [9]; no data available for  $\text{CeO}_2^+/\text{cyclo-C}_6\text{H}_8$ . [f] Reactions were not measured owing to the lack of corresponding deuterated compounds (see Experimental Section). [g] Values for corresponding perdeuterated compounds.

first approximation the operation of intermolecular kinetic-isotope effects, which may exist due to the employment of undeuterated compounds for  $M = \text{Ce}$  and deuterated ones for  $M = \text{Th}$  (see Experimental Section). For the sake of clarity, D atoms will be referred to as hydrogen in the following text.

Scheme 2 contains an overview of the reactions of  $\text{MO}_2^+$  ( $M = \text{Ce}, \text{Th}$ ) towards ethene, propene, and benzene, and a compilation of all measured rate constants is given in Table 3.



Scheme 2. Overview of the reactions of  $\text{MO}_2^+$  ( $M = \text{Ce}, \text{Th}$ ) towards ethene, propene, and benzene.

Neither of the cationic dioxides reacts with molecular hydrogen or with methane, although hydrogen abstraction would be thermochemically accessible for  $\text{ThO}_2^+$ . This finding can probably be attributed to the weak interaction of  $\text{CH}_4$  (or  $\text{H}_2$ ) with the dioxocation in the encounter complex. However, both  $\text{CeO}_2^+$  and  $\text{ThO}_2^+$  abstract a hydrogen atom as the sole observed process in their reactions with propane. Fully in line with the significantly higher  $\text{BDE}(\text{ThO}_2^+ - \text{H})$  ( $> 119.2 \text{ kcal mol}^{-1}$ , see above) as compared with the corresponding value for  $\text{CeO}_2^+$  (bracketed at  $89 \pm 10 \text{ kcal mol}^{-1}$  [9]), the reaction is measured to be much faster for  $\text{ThO}_2^+$  ( $k_{\text{rel}} = 0.13$ ) than for  $\text{CeO}_2^+$  ( $k_{\text{rel}} = 0.003$ ). In

the case of the unsaturated hydrocarbons ethene, propene, and benzene, the abstraction of a hydrogen atom again represents the major, and in the case of benzene even the exclusive pathway pursued by  $\text{ThO}_2^+$ . This radical-like behavior [26] can be explained by analogy with the Ce case: [9] a detailed theoretical investigation on the  $\text{CeO}_2^+$  cation revealed a relatively unstable electronic situation in which one unpaired electron was found to reside in a  $\sigma_u$  molecular orbital with contributions from both the oxygen  $2p_{z^2}$  and the cerium  $4f_{z^3}$  and  $5p_{z^2}$  orbitals to give rise to the  $^2\Sigma_u^+$  ground state. On the other hand, one of the oxygen ligands forms a new bond to a hydrogen atom in  $\text{CeO}(\text{OH})^+$  and a closed-shell species arises in which a double bond to the oxo ligand and a single bond to the hydroxo ligand are formed, resulting in a saturated valence shell at the singly charged Ce center. The driving force for the remarkable reactivity of  $\text{ThO}_2^+$  is provided by  $\text{BDE}(\text{ThO}_2^+ - \text{H})$ , which itself is based on the underlying electronic structures of reactant and product ions. In fact, activation of hydrocarbon substrates by a classical insertion/elimination mechanism with concomitant loss of a corresponding neutral closed-shell species can be ruled out in this case since in a simple scenario at least two nonbonding electrons are required for the insertion process; for  $\text{ThO}_2^+$  only a single unpaired electron is available. As a pathway competing with the hydrogen-atom abstraction, oxygen-atom transfer to the alkenes is observed to generate  $\text{ThO}^+$ . With respect to the reported  $\text{BDE}(\text{ThO}^+ - \text{O})$  of  $112 \pm 4 \text{ kcal mol}^{-1}$ , [21] only acetaldehyde is accessible as a neutral oxidation product in the reaction with ethene. From that result, we obtain a slightly corrected upper bracket and derive a  $\text{BDE}(\text{ThO}^+ - \text{O})$  of  $110 \pm 2 \text{ kcal mol}^{-1}$ . Upon reaction with propene, either acetone or propanal can be generated by oxygen-atom transfer. In contrast to the  $\text{ThO}_2^+$  case,  $\text{CeO}_2^+$  strongly favors the oxidation channel upon collision

with unsaturated hydrocarbons. [9] In the reactions with ethene and benzene, an oxygen atom is transferred to yield exclusively the diatomic  $\text{CeO}^+$  and the corresponding oxidized hydrocarbon, which, in the case of benzene, is phenol. Even in the reaction with propene which offers a competing pathway, namely, homolytic cleavage of the relatively weak allylic C–H bond, 75% of the reaction products correspond to the oxidation process described above. These reactivity differences between the lanthanide and the actinide dioxocations are not surprising if one considers the significantly lower BDE of the second oxygen ligand at Ce ( $88 \pm 15 \text{ kcal mol}^{-1}$ ) compared with the corresponding value of Th

( $110 \pm 2 \text{ kcal mol}^{-1}$ ). The strong second metal–oxygen bond to Th obviously disfavors oxidation of ethene as well as propene and renders it impossible for benzene, which undergoes an exothermic oxidation only with metal oxides that exhibit a  $\text{BDE}(\text{M}^+ - \text{O})$  of less than  $101.9 \text{ kcal mol}^{-1}$ .

**Reactions of metal monoxocations:** The most common oxidation state of lanthanide compounds in the condensed phase is +III, though  $\text{Ce}^{\text{IV}}$  (e.g.  $\text{CeO}_2^+$ ) plays a role in the active sites of automobile exhaust converters, and several other examples for  $\text{Eu}^{\text{II}}$  and  $\text{Yb}^{\text{II}}$  compounds are known. [27] This general preference for

the trivalent state can be traced back to the energy and the compact nature of the 4f electrons, which can be considered to belong to the lanthanide core rather than to their valence shell. In this respect, cationic lanthanide oxides  $\text{LnO}^+$  can be regarded as completely saturated species because two of the three valence electrons are involved in making a double bond to the oxygen ligand and the third one is detached upon ionization. This simple view at least holds true for the early lanthanides and is reflected by the unusually high  $\text{BDE}(\text{Ln}^+-\text{O})$  values for  $\text{Ln} = \text{La}-\text{Nd}$ .<sup>[28]</sup> Thus,  $\text{CeO}^+$  and  $\text{NdO}^+$  are, a priori, expected to be inert towards most substrates, as has been shown previously for  $\text{CeO}^+$ .<sup>[9]</sup> However, this approximate concept is no longer fully applicable as more f electrons are added along the lanthanide row. This subject, however, goes far beyond the scope of the present work and will be discussed in detail in a forthcoming paper.<sup>[29]</sup>

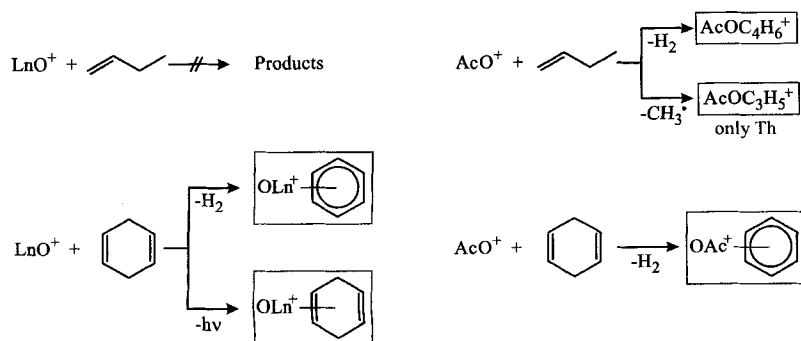
None of the metal oxides  $\text{MO}^+$  ( $\text{M} = \text{Ce}, \text{Nd}, \text{Th}, \text{U}$ ) were found to activate molecular hydrogen, methane, or propane, and they are also inert towards ethene, propene, and benzene. Nevertheless, remarkable differences in the chemical behavior of the four oxocations under investigation become apparent when higher alkenes, namely, 1-butene and 1,4-cyclohexadiene, are employed. These substrates not only possess quite weak allylic C–H bonds but also, owing to their higher polarizabilities compared with the smaller substrates, they lower the potential energy wells of the initially formed, rovibrationally excited, ion/molecule encounter complexes. Moreover, dehydrogenation of 1-butene and 1,4-cyclohexadiene leads to stable butadiene and benzene complexes, respectively, thus enhancing the exothermicity of the corresponding processes. Note, in this context, that dehydrogenation of 1,4-cyclo- $\text{C}_6\text{H}_8$  to form benzene is itself exothermic by  $6 \text{ kcal mol}^{-1}$ . These three factors significantly influence the height of activation barriers leading to products, and 1-butene and 1,4-cyclohexadiene have already been successfully employed to probe reactivity thresholds of “bare”  $\text{Ln}^+$ .<sup>[3]</sup>

Scheme 3 depicts the observed reactions of  $\text{CeO}^+$  and  $\text{NdO}^+$  with 1- $\text{C}_4\text{H}_8$  and cyclo- $\text{C}_6\text{H}_8$ . The corresponding relative reaction rates are listed in Table 3. Neither oxide reacts with 1- $\text{C}_4\text{H}_8$ . Upon reaction with cyclo- $\text{C}_6\text{H}_8$ , only 10% of the very low reaction rate ( $k_{\text{rel}} = 0.004$ ) of  $\text{CeO}^+$  is associated with formation of a benzene complex, and 90% corresponds to adduct formation. We cannot decide whether the  $\text{CeOC}_6\text{H}_6^+$  signal is due to adduct formation with benzene impurities in the cyclo- $\text{C}_6\text{H}_8$  or corresponds to a genuine chemical reaction, as the

overall process occurs close to the detection limit.  $\text{NdO}^+$ , on the other hand, does indeed dehydrogenate the cyclic alkadiene, but still at a low rate ( $k_{\text{rel}} = 0.03$ ). Only 25% of the primary products correspond to  $\text{NdOC}_6\text{H}_6^+$ , while adduct formation represents the major pathway.

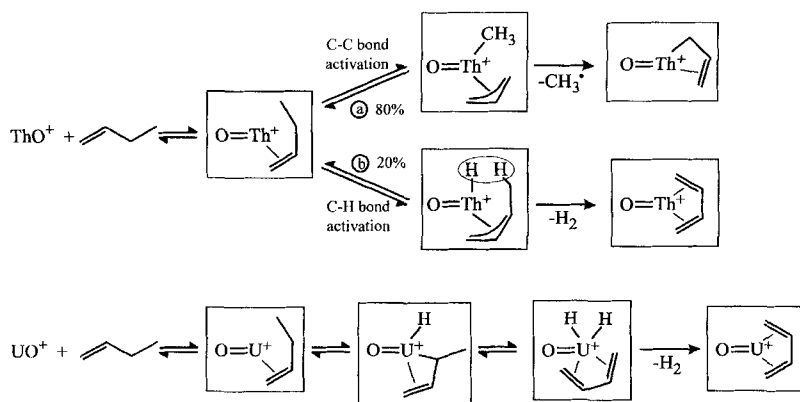
Let us, in this context, inspect the underlying electronic structures of these cationic lanthanide oxides. Unfortunately, to the best of our knowledge, no experimental data on the electronic spectra of  $\text{MO}^+$  ( $\text{M} = \text{Ce}, \text{Nd}, \text{Th}, \text{U}$ ) are available so far. Recent calculations on  $\text{CeO}^+$  by means of ab initio pseudopotential (PP) as well as density-functional methods<sup>[9]</sup> predict a  $^2\Phi$  ground state in which two out of the cationic cerium's three valence electrons form the double bond to oxygen in a “perfect pairing” pattern.<sup>[30]</sup> The third one is a nonbonded, metal-centered 4f electron of  $\phi$  symmetry. The compact nature of this SOMO is responsible for the observed inertness and justifies assignment of that electron to the core of cerium rather than to its valence shell. The ground-state configuration of  $\text{NdO}^+$  has not yet been reported, and a computational approach to  $\text{NdO}^+$  appears quite demanding and would certainly go beyond the scope of the present paper, since at least three unpaired electrons and an open f shell have to be taken into account. However, its valence structure can be easily derived from a simple model, which has already been successfully applied to calibrate predictions for  $\text{BDE}(\text{Ln}^+-\text{CH}_2)$ .<sup>[31]</sup> 1) The high  $\text{BDE}(\text{Nd}^+-\text{O}) = 178 \pm 7 \text{ kcal mol}^{-1}$  suggests, as in the case of cerium, a “perfect pairing” pattern for the neodymium–oxygen bond.<sup>[31]</sup> 2) Binding to the oxygen ligand thus requires excitation of one 4f electron into a 5d orbital from ground-state  $\text{Nd}^+$  (configuration:  $6s^1 4f^4$ ; term:  $^6I_{7/2}$ )<sup>[32]</sup> to give rise to two “active” non-valence electrons for formation of the double bond while three unpaired electrons remain in the 4f subshell.<sup>[33]</sup> 3) Upon attachment of the oxygen ligand, the effective charge on the metal center is raised, implying further stabilization of the f as compared with the s or d orbitals.<sup>[34]</sup> Within this scenario,  $\text{NdO}^+$  exhibits three “inactive” unpaired 4f electrons on the metal center and, thus should exhibit a similar inertness to  $\text{CeO}^+$ . This conclusion is supported by the experimental results, which reveal only a very low reactivity of  $\text{NdO}^+$  towards 1,4-cyclohexadiene.

Interestingly, in contrast to their lighter homologues,  $\text{ThO}^+$  and  $\text{UO}^+$  activate 1-butene (see Table 3 and Scheme 3). More than 20% of all collisions of  $\text{ThO}^+$  with 1-butene are reactive and lead to two different reaction products. In one pathway, a methyl radical is expelled from the hydrocarbon substrate to give rise to an ion of the composition  $\text{ThOC}_3\text{H}_5^+$  (80%). This radical-type behavior of  $\text{ThO}^+$  can be explained according to the mechanism depicted in Scheme 4: after initial formation of the rovibrationally excited ion/molecule encounter complex, the weak allylic C–C bond ( $\text{BDE} = 75.3 \text{ kcal mol}^{-1}$ ) is homolytically cleaved. In the intermediate thus formed, a methyl and an allyl radical are bound to  $\text{ThO}^+$ . This leads, however, to an unsatisfactory electronic situation, since only one valence electron is left on the metal center for formation of the bonds to the two open-shell fragments. Thus, from this complex, subse-



Scheme 3. Reactions of  $\text{LnO}^+$  ( $\text{M} = \text{Ce}, \text{Nd}$ ) and  $\text{AcO}^+$  ( $\text{M} = \text{Th}, \text{U}$ ) with 1- $\text{C}_4\text{H}_8$  and cyclo- $\text{C}_6\text{H}_8$ .

quent loss of either the allyl or the methyl radical is required to yield a stable ionic closed-shell product. As a matter of fact, only the latter process is observed; it leads to an ion of composition  $\text{ThOC}_3\text{H}_5^+$ , which can be regarded as an oxo-allyl complex of  $\text{Th}^+$ . In contrast to the alternative  $\text{OTh}^+-\text{CH}_3$  species,  $\text{ThOC}_3\text{H}_5^+$  is stabilized by electrostatic interaction of the metal's positive charge with the  $\pi$ -electron system of the organic residue. In the second pathway, the butadiene complex  $\text{OThC}_4\text{H}_6^+$  is formed (Scheme 4, pathway b, 20%) through loss



Scheme 4. Mechanisms of reactions of  $\text{ThO}^+$  and  $\text{UO}^+$  with 1- $\text{C}_4\text{H}_8$ .

of a hydrogen molecule. Following pathway b,  $\text{ThO}^+$  abstracts an allylic H atom from 1-butene ( $\text{BDE} = 82.3 \text{ kcal mol}^{-1}$ ), giving rise to an intermediate analogous to the one formed in pathway a. However, direct loss of a single hydrogen atom is energetically disfavored in comparison with the expulsion of a methyl radical. Thus,  $\text{H}^\cdot$  abstracts one of the remaining H atoms on the substrate, and consequently a hydrogen molecule is lost to give rise to the butadiene complex. The latter process finds its counterpart in several examples of organic radical cation chemistry.

To correlate these experimental findings with the underlying electronic structure of the thorium oxocation, we have calculated ground and low-lying excited states for  $\text{ThO}^+$  using the CCSD(T) and additional CASSCF methods. The latter was employed to obtain access to the first excited state with a major contribution from a 5f orbital to the SOMO ( ${}^2\Phi$ ). This state exhibits the same  $B_1 + B_2$  symmetry within the  $C_{2v}$  point group—the largest abelian subgroup to the  $C_{\infty v}$  molecular symmetry available in MOLPRO—as the corresponding SOMO with a major 5d contribution ( ${}^2\Pi$ ). Term energies and equilibrium distances are given in Table 4.  $\text{BDE}(\text{Th}^+-\text{O})$  was calculated within the CCSD(T) scheme to  $196.3 \text{ kcal mol}^{-1}$  and is in

Table 4. Equilibrium bond lengths  $r_e$  (in Å) and adiabatic and vertical term energies  $T_e$  (in  $\text{cm}^{-1}$ ) of low-lying states of  $\text{ThO}^+$ .

Term	$r_e$	CCSD(T)		CASSCF $T_e$ (vertical)
		$T_e$ (adiabatic)	$T_e$ (vertical)	
${}^2\Sigma$	1.829	0	0	0
${}^2A$	1.842	5267	5299	4111
${}^2\Pi$	1.850	11798	11880	11213
${}^2\Phi$ [a]	–	–	–	22029

[a] These values are not accessible with the CCSD(T) method since both  ${}^2\Pi$  and  ${}^2\Phi$  terms transform to the same  $B_1 + B_2$  irreducible representations in the  $C_{2v}$  point group.

reasonable agreement with the experimental value of  $209 \pm 4 \text{ kcal mol}^{-1}$ . This accuracy is satisfactory for the present purpose, which is to give a picture of the relative order of low-lying excited states rather than numerically accurate spectroscopic constants. In this context, the agreement between CCSD(T) and CASSCF term energies is satisfactory. It is found that one metal-centered single electron corresponding to the 7s atomic orbital of thorium gives rise to the  ${}^2\Sigma^+$  ground state of  $\text{ThO}^+$ . The lowest-lying excited state in which the unpaired

electron has mainly f-character ( ${}^2\Phi$ ) has a term energy as high as  $22029 \text{ cm}^{-1}$  (CASSCF), which prevents its population under the thermal conditions that prevail in the FT-ICR. The pure s character of the unpaired electron in ground-state  $\text{ThO}^+$  is in line with earlier computational results for neutral  $\text{ThO}$ ,<sup>[35]</sup> where the  ${}^1\Sigma^+$  ground state has been pictured as  $\text{Th}^{2+}(7s^2, {}^1S)\text{O}^{2-}({}^1S)$ . These theoretical findings corroborate the surprising gas-phase reactivity of  $\text{ThO}^+$  in its reactions with 1-butene and water.

$\text{UO}^+$ , on the other hand, reacts differently: at a much slower rate ( $k_{\text{rel}} = 0.008$ ) than  $\text{ThO}^+$ , single dehydrogenation is pursued exclusively in the reaction with 1-butene. The fact that loss of a methyl radical is not observed suggests a completely different mechanism to be operative here. Based on

analogous considerations to those outlined above for  $\text{NdO}^+$ , binding of an oxygen ligand to  $\text{U}^+$  (ground-state configuration  $7s^2 5f^3$ ; term  ${}^4I_{9/2}$ )<sup>[38]</sup> is expected to give rise to an oxocation  $\text{UO}^+$  with three unpaired nonbonding electrons of 5f character. In fact, earlier SCF and MC-SCF PP calculations on  $\text{UO}^+$  predict an  ${}^4I_{9/2}$  ground state dominated by the single  $A = 6$  function. It was found that the ground state is very ionic with substantially localized molecular orbitals, which at best can be described as  $\text{U}^{3+}(5f^3, {}^4I)\text{O}^{2-}({}^1S)$ .<sup>[36]</sup> In addition, experimental (PES) as well as theoretical results on neutral  $\text{UO}$ <sup>[37]</sup> describe its electronic ground state as resulting from a  $7s^2 5f^2$  configuration on uranium. This illustrates the general tendency for the energy of f orbitals to be lowered with rising charge on the metal, and thus supports the assumptions we made for the ground state of  $\text{NdO}^+$ .

The three unpaired electrons on  $\text{UO}^+$  (see below) open up the possibility of a reaction with an insertion/elimination mechanism as depicted in Scheme 4. Instead of abstracting an allylic H atom,  $\text{UO}^+$  is able to insert into the corresponding C–H bond. Subsequent  $\beta$ -hydrogen shift leads to an oxo-dihydrobutadiene complex, which, by loss of  $\text{H}_2$ , yields the product ion  $\text{OUC}_4\text{H}_6^+$ . Loss of exchange energy among the unpaired electrons upon formation of U–H and U–C bonds leads to a relative destabilization of the intermediates, and thus accounts for the inefficiency of the corresponding process in contrast to the  $\text{ThO}^+$  case.

When the significantly more polarizable substrate 1,4-cyclohexadiene is employed, effective dehydrogenation is the only process observed for both  $\text{ThO}^+$  ( $k_{\text{rel}} = 0.75$ ) and  $\text{UO}^+$  ( $k_{\text{rel}} = 0.51$ ). This enhanced reactivity is not surprising, since deepening of the potential energy wells in the initially formed ion/molecule complexes lowers the barriers en route to the products, and thus accelerates the corresponding C–H bond activa-

tion processes. In contrast to 1-butene, C–C bond activation of the cyclic substrate by  $\text{ThO}^+$  does not occur, owing to the ease of dehydrogenation and the lack of allylic C–C bonds in 1,4-cyclohexadiene.

**Comparison of  $\text{LnO}_n^+$  and  $\text{AcO}_n^+$  ( $n = 0-2$ ):** In this concluding section, we compare the reactivity of the “bare” metal ions with their corresponding oxo complexes with regard to the following questions: 1) How does addition of one or two oxygen ligands influence the chemical properties of f elements? 2) Can a general differentiation between the gas-phase chemistry of lanthanides and actinides be made? 3) What is the role of f electrons in the chemistry of  $\text{Ln}^+$  and  $\text{An}^+$  cations?

The reactivity of “bare”  $\text{Ln}^+$  towards hydrocarbons can be summarized as follows. Only closed-shell neutral species, mainly molecular hydrogen, are lost from the reacting substrates. The processes observed obey a classical insertion/elimination mechanism. The measured reaction rates of  $\text{Ln}^+$  depend on the excitation energies from the respective electronic ground state to a state with two non-f valence electrons, the latter being required for insertion into a C–H or C–C bond.<sup>[3]</sup> In this respect, it appears natural that  $\text{Ce}^+$  ( $6s^0 5d^2 4f^1$  ground-state configuration),<sup>[32]</sup>  $\text{Th}^+$  ( $7s^1 6d^2 5f^0$ ),<sup>[38]</sup> and  $\text{U}^+$  ( $7s^2 6d^0 5f^3$ )<sup>[38]</sup> react at similar rates with butane as well as with all unsaturated hydrocarbons investigated (see Table 3). However, the remarkable differences observed for the lower alkanes deserve a closer look. Reactions of  $\text{Ln}^+$  with methane were not observed on thermochemical grounds, whereas slow formation of  $\text{ThCH}_2^+$  ( $k_{\text{rel}} = 0.04$ ) suggests that this reaction proceeds close to the thermochemical threshold. The corresponding process is not observed for  $\text{U}^+$ , since here the potential product  $\text{UCH}_2^+$  is expected to be destabilized in comparison with the thorium complex by the greater loss of exchange energy. The same argument applies for the reaction with propane, which proceeds at moderate efficiencies for  $\text{Ce}^+$  ( $k_{\text{rel}} = 0.30$ ) and  $\text{Th}^+$  ( $k_{\text{rel}} = 0.65$ ), whereas it is slow for  $\text{U}^+$  ( $k_{\text{rel}} = 0.02$ ). Note, in addition, that  $\text{Th}^+$  dehydrogenates ethane more efficiently ( $k_{\text{rel}} = 0.40$ ) than its lighter homologue  $\text{Ce}^+$  ( $k_{\text{rel}} = 0.005$ ) in analogy with the different reactivity of transition metals from the first d period and those of the second and third.<sup>[39]</sup>

For the evaluation of the effect of the first oxygen ligand, it is instructive to consider the underlying electronic structures of  $\text{MO}^+$ . The overall inertness of  $\text{CeO}^+$  can be attributed to its  $^2\Phi$  electronic ground state, the SOMO of which arises from a 4f atomic orbital. In contrast, the corresponding actinide compound,  $\text{ThO}^+$  ( $^2\Sigma^+$ ), exhibits radical-like reactivity, as evidenced by the strong bias towards loss of  $\text{CH}_3$  from 1-butene. With respect to its active unpaired electron of s character,  $\text{ThO}^+$  has to be regarded as the cationic oxide of a d element rather than of an f element. To confirm this hypothesis, the reactions of 1-butene and 1,4-cyclohexadiene with  $\text{ZrO}^+$  were measured under identical experimental conditions, because the ground state of  $\text{ZrO}^+$  has been experimentally determined to exhibit the same symmetry<sup>[40]</sup> ( $^2\Sigma^+$  with a nonbonding 5s electron on the metal center) as the calculated ground state of  $\text{ThO}^+$ . Although activation of 1-butene by  $\text{ZrO}^+$  proceeds at the collisional limit and is therefore significantly faster than for  $\text{ThO}^+$ , the same product channels are pursued at identical branching ratios within the accuracy of the experiment: 60% of the collisions lead to

loss of  $\text{CH}_3$  with formation of  $\text{ZrOC}_3\text{H}_5^+$  (70% for  $\text{ThO}^+$ ), and in the other collisions the butadiene complex  $\text{OZrC}_4\text{H}_6^+$  (40%) is formed by dehydrogenation of the substrate (30% for  $\text{ThO}^+$ ). Finally, the behavior of  $\text{ZrO}^+$  towards 1,4-cyclohexadiene exactly parallels the results obtained for  $\text{ThO}^+$ : molecular hydrogen is lost at the collision limit to yield the  $\text{OZrC}_6\text{H}_6^+$  product ion exclusively.

Within the scenario outlined in the preceding section, the assumption that both  $\text{NdO}^+$  and  $\text{UO}^+$  exhibit three unpaired f electrons in their ground state seems justified, and therefore these two ions represent suitable model systems to probe 4f versus 5f electron reactivity. Not unexpectedly, the 4f electrons of  $\text{NdO}^+$  do not allow a reaction with 1-butene and even 1,4-cyclohexadiene is only very slowly dehydrogenated. The 5f electrons on  $\text{UO}^+$ , on the other hand, do indeed induce slow dehydrogenation of 1-butene, and the corresponding process becomes efficient when the diene is used; this provides evidence for the participation of 5f electrons in bond formation during activation processes.

In line with the arguments outlined above, upon attachment of the second oxygen ligand to  $\text{UO}^+$  the single 5f electron left on the uranium center in  $\text{UO}_2^+$  becomes lower in energy and more compact, rendering this dioxide inert. The similarity of  $\text{ThO}_2^+$  and  $\text{CeO}_2^+$  in their gas-phase behavior towards the various hydrocarbon substrates investigated can be traced back to similar electronic structures in which participation of f orbitals plays a negligible role. Their chemistry is determined by their radical character, which is due to an electron hole in the valence shell, as well as by the BDE( $\text{OM}^+ - \text{O}$ ). Significant differences in the latter account for the observed variations in branching ratios of H-atom abstraction versus O-atom transfer processes.

**Acknowledgments:** Financial support by the Bundesministerium für Bildung, Wissenschaft, Forschung und Technologie, the Deutsche Forschungsgemeinschaft, the Volkswagen-Stiftung, and the Fonds der Chemischen Industrie is acknowledged. We are grateful to Dr. Jeremy Harvey, Dr. Detlef Schröder, and Dipl.-Chem. Wolfgang Kühle for helpful discussions. H. S. and H. H. C. thank Prof. Antonio Pires de Matos and Dr. Joaquim Marçalo for an ongoing fruitful collaboration on gas-phase chemistry of f-elements and for their hospitality during stays at the Instituto Tecnológico e Nuclear, Sacavém.

Received: January 29, 1997 [F590]

- [1] Recent reviews: a) P. B. Armentrout, *Annu. Rev. Phys. Chem.* **1990**, *41*, 313. b) J. A. Martinho Simões, J. L. Beauchamp, *Chem. Rev.* **1990**, *90*, 629. c) K. Eller, H. Schwarz, *ibid.* **1991**, *91*, 1121. d) J. C. Weishaar, *Acc. Chem. Res.* **1993**, *26*, 213. e) B. S. Freiser, *ibid.* **1994**, *27*, 353.
- [2] a) Y. Huang, M. B. Wise, D. B. Jacobson, B. S. Freiser, *Organometallics* **1987**, *6*, 346. b) R. L. Hettich, B. S. Freiser, *J. Am. Chem. Soc.* **1987**, *109*, 3543. c) J. B. Schilling, J. L. Beauchamp, *ibid.* **1988**, *110*, 15. d) L. S. Sunderlin, P. B. Armentrout, *ibid.* **1989**, *111*, 3845. e) Y. Huang, Y. D. Hill, B. S. Freiser, *ibid.* **1991**, *113*, 840. f) Y. A. Ranasinghe, T. J. MacMahon, B. S. Freiser, *ibid.* **1992**, *114*, 9112. g) Y. A. Ranasinghe, B. S. Freiser, *Chem. Phys. Lett.* **1992**, *200*, 135. h) M. Azarro, S. Breton, M. Decouzon, S. Geribaldi, *Int. J. Mass Spectrom. Ion Processes* **1993**, *128*, 1.
- [3] a) W. W. Yin, A. G. Marshall, J. Marçalo, A. Pires de Matos, *J. Am. Chem. Soc.* **1994**, *116*, 8666. b) H. H. Cornehl, C. Heinemann, D. Schröder, H. Schwarz, *Organometallics* **1995**, *14*, 992. c) J. K. Gibson, *J. Phys. Chem.* **1996**, *100*, 15688.
- [4] J. Marçalo, J. P. Leal, A. Pires de Matos, *Int. J. Mass Spectrom. Ion Processes* **1996**, *158*, 265.
- [5] C. Heinemann, H. H. Cornehl, H. Schwarz, *J. Organomet. Chem.* **1995**, *501*, 201.
- [6] See, for example: a) B. L. Tjelta, P. B. Armentrout, *J. Am. Chem. Soc.* **1995**, *117*, 5531. b) P. A. M. van Koppen, J. E. Bushnell, P. R. Kemper, M. T. Bowers, *J. Am. Chem. Soc.* **1995**, *117*, 2098. c) D. Schröder, H. Schwarz, *J. Organomet. Chem.* **1995**, *504*, 123, and references therein.

- [7] D. Schröder, H. Schwarz, *Angew. Chem. Int. Ed. Engl.* **1995**, *34*, 1973.
- [8] See, for example: a) K. K. Irikura, J. L. Beauchamp, *J. Am. Chem. Soc.* **1989**, *111*, 75. b) C. J. Cassady, S. W. McElvany, *Organometallics* **1992**, *11*, 2367. c) A. Fiedler, I. Kretzschmar, D. Schröder, H. Schwarz, *J. Am. Chem. Soc.* **1996**, *118*, 9941.
- [9] C. Heinemann, H. H. Cornehl, D. Schröder, M. Dolg, H. Schwarz, *Inorg. Chem.* **1996**, *35*, 2463.
- [10] a) K. Eller, H. Schwarz, *Int. J. Mass Spectrom. Ion Processes* **1989**, *93*, 243. b) K. Eller, W. Zummack, H. Schwarz, *J. Am. Chem. Soc.* **1990**, *112*, 621.
- [11] a) B. S. Freiser, *Talanta* **1982**, *32*, 697. b) B. S. Freiser, *Anal. Chim. Acta* **1985**, *178*, 137.
- [12] R. A. Forbes, F. H. Laukien, J. Wronka, *Int. J. Mass Spectrom. Ion Processes* **1988**, *83*, 23.
- [13] A. J. R. Heck, L. J. de Koning, F. A. Pinske, N. M. M. Nibbering, *Rap. Commun. Mass Spectrom.* **1991**, *5*, 406.
- [14] T. Su, M. T. Bowers, *Int. J. Mass Spectrom. Ion Phys.* **1973**, *12*, 347.
- [15] a) R. C. Burnier, R. B. Cody, B. S. Freiser, *J. Am. Chem. Soc.* **1982**, *104*, 7436. b) R. B. Cody, B. S. Freiser, *Int. J. Mass Spectrom. Ion Phys.* **1982**, *41*, 199.
- [16] W. Küchle, M. Dolg, H. Stoll, H. Preuss, *J. Chem. Phys.* **1994**, *100*, 7535.
- [17] P.-O. Widmark, B. J. Persson, B. O. Roos, *Theor. Chim. Acta* **1991**, *79*, 419.
- [18] MOLPRO is a package of ab initio programs written by H.-J. Werner, P. J. Knowles, with contributions from J. Almlöf, R. D. Amos, M. J. O. Deegan, S. T. Elbert, C. Hampel, W. Meyer, K. Peterson, R. Pitzer, A. J. Stone, P. R. Taylor.
- [19] P. J. Knowles, C. Hampel, H.-J. Werner, *J. Chem. Phys.* **1993**, *99*, 5219.
- [20] M. C. R. Cockett, L. Nyulászi, T. Veszprémi, T. G. Wright, J. M. Dyke, *J. Electron Spectrosc. Relat. Phenom.* **1991**, *57*, 373.
- [21] a) S. G. Lias, J. E. Bartmess, J. F. Liebman, J. L. Holmes, R. D. Levin, W. G. Mallard, *Gas-Phase Ion and Neutral Thermochemistry*, *J. Phys. Chem. Ref. Data*, Suppl. 1, **1988**. b) S. G. Lias, J. F. Liebman, R. D. Levin, S. A. Kafafi, *NIST Standard Reference Database, Positive Ion Energetics*, Version 2.01, Gaithersburg, MD, January **1994**.
- [22] For a recent example, see: a) A. Fiedler, D. Schröder, S. Shaik, H. Schwarz, *J. Am. Chem. Soc.* **1994**, *116*, 10734. b) D. E. Clemmer, Y.-M. Chen, F. A. Khan, P. B. Armentrout, *J. Phys. Chem.* **1994**, *98*, 6522.
- [23] H. H. Cornehl, C. Heinemann, J. Marçalo, A. Pires de Matos, H. Schwarz, *Angew. Chem. Int. Ed. Engl.* **1996**, *35*, 891.
- [24] For a detailed description of the spectrometer see: a) R. Srinivas, D. Sülzle, T. Weiske, H. Schwarz, *Int. J. Mass Spectrom. Ion Processes* **1991**, *107*, 368. b) R. Srinivas, D. Sülzle, W. Koch, C. H. DePuy, H. Schwarz, *J. Am. Chem. Soc.* **1991**, *113*, 5970. For a brief summary of the experimental procedure, see ref. [23].
- [25] H. H. Cornehl, G. Hornung, H. Schwarz, unpublished results.
- [26] For a related recent example, see: M. F. Ryan, A. Fiedler, D. Schröder, H. Schwarz, *J. Am. Chem. Soc.* **1995**, *117*, 2033.
- [27] H. Schumann, J. A. Meese-Marktscheffel, L. Esser, *Chem. Rev.* **1995**, *95*, 865, and references therein.
- [28] BDE(Ln<sup>+</sup>-O) in kcalmol<sup>-1</sup> according to ref. [20]: La = 203 ± 7; Ce = 196 ± 16; Pr = 189 ± 7; Nd = 178 ± 7.
- [29] H. H. Cornehl, R. Wesendrup, J. N. Harvey, H. Schwarz, *J. Chem. Soc. Perkin Trans. 2*, submitted.
- [30] a) S. Shaik, D. Danovich, A. Fiedler, D. Schröder, H. Schwarz, *Helv. Chim. Acta* **1995**, *78*, 1393. b) see also ref. [22].
- [31] Electronic excitation energy in conjunction with loss of exchange energy upon bond formation reflects the lower BDE(Nd<sup>+</sup>-O) compared with BDE(Ce<sup>+</sup>-O). For details, see ref. [3].
- [32] W. C. Martin, R. Zalubas, L. Hagan, *Atomic Energy Levels—The Rare Earth Elements*; NSRDS-NBS 60, National Bureau of Standards, Washington, DC, **1978**.
- [33] The validity of this so-called promotional model has already been established for the neutral rare-earth monoxides, and for NdO a 4f<sup>3</sup> valence configuration on the metal center has been predicted: M. Dolg, H. Stoll, *Theor. Chim. Acta* **1989**, *75*, 369, and references therein.
- [34] See for example: M. Dolg, H. Stoll, in *Handbook on the Physics and Chemistry of Rare Earths*, Vol. 22 (Eds.: K. A. Gschneider, Jr., L. Eyring), Elsevier, B. V., Amsterdam, **1996**, pp. 3 and references therein.
- [35] W. Küchle, M. Dolg, H. Stoll, H. Preuss, *J. Chem. Phys.* **1994**, *100*, 7535.
- [36] M. Krauss, W. J. Stevens, *Chem. Phys. Lett.* **1983**, *99*, 417.
- [37] G. C. Allen, E. J. Baerends, P. Vernooijs, J. M. Dyke, A. M. Ellis, M. Fehé, R. A. Morris, *J. Chem. Phys.* **1988**, *89*, 5363.
- [38] J. Blaise, J.-F. Wyart in *International Tables of Selected Constants*, Vol. 20: *Tables Internationales de Constantes*, Paris, **1992**.
- [39] See, for example: a) M. A. Tolbert, M. L. Mandlich, L. F. Halle, J. L. Beauchamp, *J. Am. Chem. Soc.* **1986**, *108*, 5675. b) R. Wesendrup, C. A. Schalley, D. Schröder, H. Schwarz, *Chem. Eur. J.* **1995**, *1*, 608.
- [40] a) W. J. Balfour, B. Lindgren, *Phys. Scr.* **1980**, *22*, 36. b) R. J. Van Zee, S. Li, W. Weltner, Jr., *Chem. Phys. Lett.* **1994**, *217*, 381